Understanding the Relationship between Surface Coverage and Molecular Orientation in Polar Self-Assembled Monolayers

C. Thomas Buscher, Duncan McBranch, and DeQuan Li*

Contribution from the Chemical Science and Technology Division, Los Alamos National Laboratory, Los Alamos, New Mexico 87545

Received August 21, 1995[⊗]

Abstract: We report here a study of surface coverage and molecular orientation in polar self-assembled monolayers (SAMs). The ordering in these SAMs arises from the competition of bonding to the surface and mutual steric effects that force alignment of the dipolar chromophores. The optimized molecular orientation was found to be 32 ± 3°, and the maximum surface coverage was approximately 2−4 molecules per nm^2 depending on the molecular cross section. Second harmonic generation (SHG) measurements were performed to verify the polar alignment; transmission electron microscopy (TEM) was employed to determine the monolayer thin-film thickness (4.3 nm) in a selected SAM.

Introduction

The science of self-assembly (SA)—a phenomenon in which a supramolecular hierarchical organization or ordering is spontaneously established in complex systems without external intervention—has exploded in the past decade.[1] However, most current strategies to SA are *ad hoc*, with little understanding of the structure−function relationship and mesoscale ordering. The key fundamental issues are (1) the surface coverage *monolayers vs aggregates*, (2) the mesoscale structure *ordered vs random*, and (3) the intrinsic relationship between molecular orientation and surface coverage. By using linear and nonlinear optical spectroscopy and transmission electron microscopy (TEM), we have demonstrated that the formation of molecular self-assemblies on surfaces results from a complex interplay between chemical bonding to the surface and steric interactions of adjacent molecules.

To compare their quality, self-assembled monolayers (SAMs) consisting of 3-aminopropyl moieties on silica were prepared by (1) immersion in a 1% (v/v) solution of (3-aminopropyl)-trimethoxysilane (APTMS) in refluxing toluene[2] and (2) exposure to a vapor of refluxing 0.1−10% (v/v) APTMS in toluene.[3] Both methods have been widely used to generate silane coupling reagents on surfaces.[2,3] Finally, an indirect route to 4-aminobutyl species on surfaces was obtained by anchoring (3-cyanopropyl)trichlorosilane (3.2 mM, $CHCl_3$) to the oxide surface, followed by $LiAlH_4$ reduction in THF.[4] The amino terminated surfaces were then phosphorylated with $POCl_3$, followed by zirconation ($ZrOCl_2$(aq)) or hafnation ($HfOCl_2$(aq)). We have found that $HfOCl_2$ is a stronger binder to phosphonate than $ZrOCl_2$, but we have used $ZrOCl_2$ for most of our studies because it provides adequate bonding strength.

Experimental Section

The fused quartz substrates were cut into sizes of 10 × 40 mm then ultrasonically cleaned in 10% detergent solution for 10 min. The substrates were refluxed in 1% tetrasodium ethylenediaminetetraacetate solution for 10 min, followed by another 10-min sonication at ambient temperature. Finally, the substrates were thoroughly rinsed with deionized water and acetone, then sputter cleaned using an argon plasma at 0.5 Torr for more than 30 min.

Formation of the chromophoric sulfonate SAMs consisted of four primary steps: (1) preparation of amino-terminated SAMs, (2) phosphorylation, (3) zirconation or hafnation, and (4) coordination of various sulfonate dyes to the zirconium anchor. Silane-based SAMs of various qualities can be formed while using typical preparation conditions reported in the literature. The chromophoric sulfonates include 1,4-bishydroxy-1,1′-azobenzene-4′-sulfonic acid, sodium salt (Tropaeolin); 4-amino-1,1′-azobenzene-3,4′-disulfonic acid, sodium salt (AABDS); 4-(4-hydroxy-1-naphthylazo)benzenesulfonic acid, sodium salt (Orange I); 4″-nitrobenzene-1″,4-diazoamino-1,1′-azobenzene-2″-arseno-4′-sulfonic acid, sodium salt (Sulfarsazene); 4-(4-aminophenylazo)phenylarsonic acid, monosodium salt (APAPA); 5-(4-sulfophenylazo)-salicyclic acid, disodium salt (Mordant Yellow 10); tetrasulfonic phthalocyanine nickel (NiPc); and α,β,γ,δ-tetrakis(5-sulfothienyl)-porphine {T(5-ST)P}.

(1) Amino-Terminated SAMs. (a) Direct Method A. The clean quartz substrates were immersed in a toluene solution containing 1% (v/v) of (3-aminopropyl)trimethoxysilane (APTMS). The system was heated to reflux overnight (∼15 h). After the reaction, the substrates were transferred into a neat $CHCl_3$ solution and cleaned by 1-min of sonication. This procedure was repeated four times. The amino-terminated SAMs were rinsed by acetone and dried in air.

(b) Direct Method B. The clean quartz substrates were clamped and suspended above the solution which contained 0.1−10% (v/v) of APTMS in toluene. The solution was heated up to refluxing temperature so that the substrates were incubated in the steam of toluene and APTMS vapors. After 2 h, the vapor deposition process was stopped and the substrates were transferred into a neat $CHCl_3$ solution and cleaned by 1-min of sonication. This procedure was repeated four times. The amino-terminated SAMs were rinsed by acetone and dried in air.

(c) Indirect Method C. The clean quartz substrates were treated with 3.2 mM (3-cyanopropyl)trichlorosilane in dry $CHCl_3$ solution for

[⊗] Abstract published in *Advance ACS Abstracts,* February 15, 1996.

(1) (a) Ulman, A. *An Introduction to Ultrathin Organic Films: from Langmuir−Blodgett to Self-Assembly*; Academic Press: Boston, 1991, and references therein. (b) Linford, M. R.; Fenter, P.; Eisenberger, P. M.; Chidsey, C. E. D. *J. Am. Chem. Soc.* **1995**, *117*, 3145−55. (c) Xia, Y.; Whitesides, G. M. *J. Am. Chem. Soc.* **1995**, *117*, 3274−75. (d) Marks, T. J.; Ratner, M. A. *Angew. Chem., Int. Ed. Engl.* **1995**, *34*, 155−73. (e) Schierbaum, K. D.; Weiss, T.; Thoden van Velzen, E. U.; Engbersen, J. F. J.; Reinhoudt, D. N..; Göpel, W. *Science* **1994**, *265*, 1413. (f) Koshland, D. E., Jr. Frontiers in Materials Science. In *Science* **1992**, *255*, 1098, special issue devoted to Self-Assembly and Biomaterials—Biomimetics, and references therein. (g) Dulcey, C. S.; Georger, J. H., Jr.; Krauthhamer, V.; Stenger, D. A.; Farer, T. L.; Calvert, J. M. *Science* **1991**, *252*, 551.

(2) (a) Chen, K.; Caldwell, W. B.; Mirkin, C. A. *J. Am. Chem. Soc.* **1993**, *135*, 1193−4. (b) Katz, H. E.; Scheller, G.; Putvinski, T. M.; Schilling, M. L.; Wilson, W. L.; Chidsey, C. E. *Science* **1991**, *254*, 1485.

(3) (a) Haller, I. *J. Am. Chem. Soc.* **1978**, *100*, 8050. (b) Zhang, X.; Gao, M.; Kong, X.; Sun, Y.; Shen, J. *J. Chem. Soc., Chem. Commun.* **1994**, 1055.

(4) Balachander, N.; Sukenik, C. N. *Langmuir* **1990**, *6(11)*, 1621−7.

0002-7863/96/1518-2950$12.00/0

Scheme 1

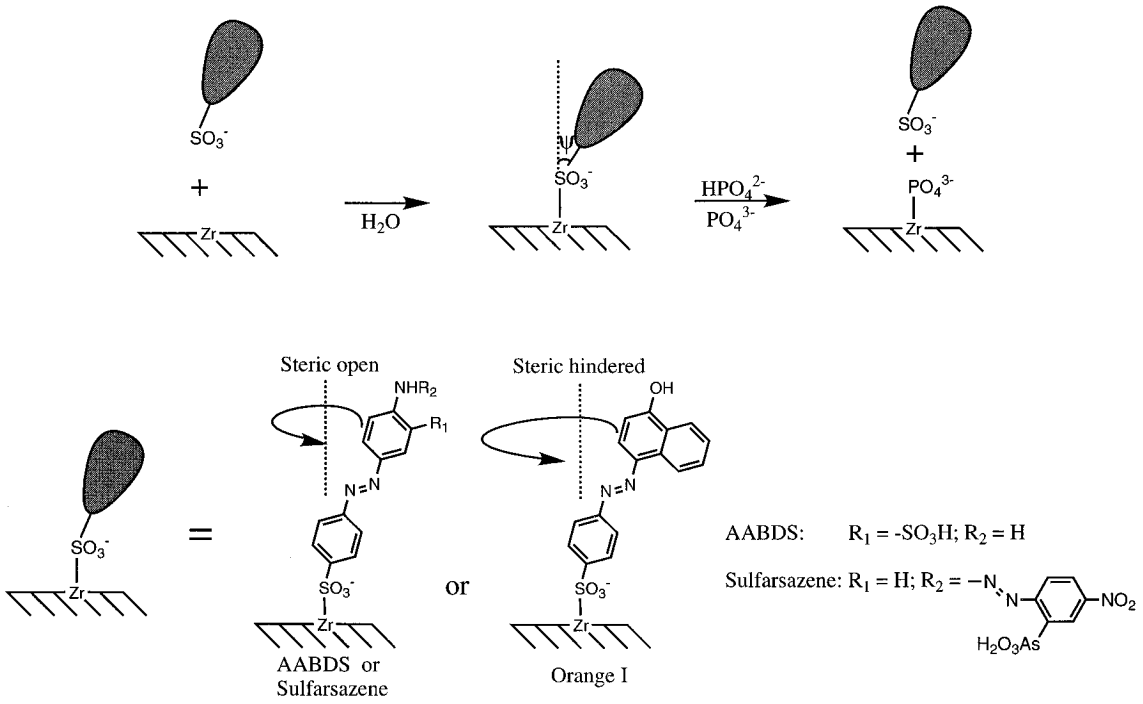

6 h. After cleaning, the cyano-terminated SAMs were immersed in a THF solution saturated with $LiAlH_4$ in a Schlenk vial overnight. After the reaction, the substrates were cleaned by sonication in THF, followed by rinsing with H_2O. The substrates were then treated with dilute HCl (10%, aqueous) solution for 10 min, followed by rinsing with deionized water. Finally, the substrates were placed in a dry triethylamine solution in an oven-dried vial for 2 h, followed by rinsing with $CHCl_3$. The final amino-terminated SAMs were dried in air.

(2) Phosphorylation of Amino-Terminated SAMs. The amino-terminated SAMs were immersed in a freshly prepared acetonitrile solution of 0.2 M phosphorus oxychloride and 0.2 M colidine for 10 min at room temperature. The phosphorylated substrates were cleaned by repeated sonication first in acetonitrile and second in water as described above. After cleaning, the substrates were thoroughly rinsed with acetone and dried in air.

(3) Phosphorylated SAMs. (a) Zirconation. The zirconated surfaces of quartz substrates were prepared by immersing the phosphorylated surfaces in a 5 mM aqueous solution of zirconyl chloride at room temperature for 10−30 min. The substrates were cleaned by repeated sonication in water as described above. The zirconated SAMs were rinsed by acetone and dried in air.

(b) Hafnation. Same as **3a** except $HfOCl_2$ was used.

(4) General Procedure for the Formation of Chromophoric Sulfonate SAMs. The zirconated surfaces were used to anchor various chromophoric sulfonate salts by immersing the substrates in a 1−5 mM aqueous solution of the corresponding chromophores. The substrates were incubated in the sulfonate dyes for 10−30 min and cleaned by repeated sonication in water as described above. The polar chromophoric SAMs were rinsed by acetone and dried in air.

(5) General Procedure for Disassembling Sulfonic Chromophores. The chromophoric SAMs were replaced with phosphonates by immersing the substrates coated with various sulfonic chromophores in a 0.1 M Na_3PO_4 and 0.1 M Na_2HPO_4 buffer solution. To assure complete exchange, the substrates were kept in the buffer for 10−30 min, cleaned by rinsing with water and then acetone, and dried in air.

(6) Molecular Orientation Determined by Surface and Solution Absorptions. In order to calculate the molecular orientation, the absorbance of both surface species and solution species must be determined accurately. Because the absorptivities of these azobenzene dyes are sensitive to pH, the absorbance measurements of the final sulfonate dye solution were carried out in a phosphate pH 11 buffer. While comparing the absorbance of surface-bound species (A_{surf}) with that of solution species (A_{soln}), the value of the absorbance of surface-bound species must be calibrated against the phosphate pH 11 buffer so that the pH-dependence effect of absorptivity of these sulfonic chromophores can be corrected.

(7) Second Harmonic Generation (SHG). SHG measurements were performed using a mode-locked (Coherent Antares), regeneratively amplified (Quantel) Nd:YAG laser with 30-Hz repetition rate, at a fundamental wavelength of 1064 nm. The second harmonic signal at 532 nm was measured as a function of angle of incidence from 0 to 80°, using a thermoelectric-cooled photomultiplier tube coupled to a boxcar integrator (Stanford Research SR250). Harmonic interference (Oriel) and colored glass (Schott BG39) filters were used to ensure that no light at the fundamental wavelength was detected.

(8) TEM Imaging. SAMs of nickel phthalocyanine (NiPc) were sandwiched for cross-sectional TEM specimen preparation using a standard procedure[7] consisting of gluing, cutting, mechanical polishing, dimpling, and ion milling. Electron microscopy was carried out using a Philips-CM30 analytical electron microscope and a Philips-CM30ST high-resolution electron microscope (HREM), both operated at 300 kV.

Results and Discussion

Analogous to Mallouk's zirconium−phosphonate surface chemistry,[5] we have employed a zirconium−sulfonate linkage which allows the convenient qualitative exchange with phosphate salts upon exposure to a phosphate buffer (Scheme 1). The zirconated surfaces were "developed" by anchoring various sulfonate chromophores including azobenzene derivatives. These azobenzene chromophores can be considered as rigid rod-like sensitizers with a charge transfer state in the blue-to-red region of the optical spectrum. The optical transition dipole moment is approximately parallel to the rigid-rod direction and can be excited only when the external electromagnetic radiation has a non-zero **E** field along the molecular axis.[6] The average angle $\langle\psi\rangle$ of the transition moments with respect to the surface normal can be derived by comparing the absorbance of the thin

(5) (a) Hong, H. G.; Sackett, D. D.; Mallouk, T. E. *Chem. Mater.* **1991**, *3*, 521−7. (b) Lee, H.; Kepley, L. J.; Hong, H. G.; Mallouk, T. E. *J. Am. Chem. Soc.* **1988**, *110*, 618−620.

(6) Perkampus, H. H. *UV-VIS Spectroscopy and Its Applications*; Springer-Verlag: New York, 1992.

(7) Edington, J. W. *Practical Electron Microscopy in Materials Science*; Macmillan: London, 1975.

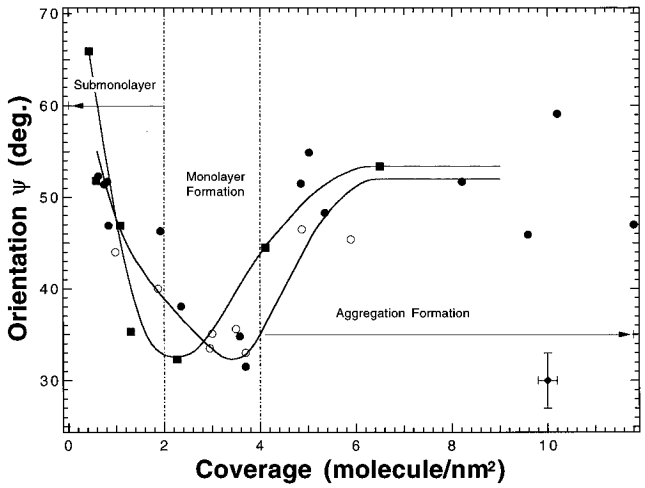

Figure 1. Plot of molecular orientation (optical transition moment) in degrees with respect to surface normal versus chromophoric monolayer coverage in units of molecules per nm^2 for AABDS (solid circles), Sulfarsazene (open circles), and Orange I (solid squares). The solid lines serve only as a visual aid.

film for light polarized parallel to the surface (A_{surf}) against that for the same number of identical species in solution (A_{soln}). Assuming a narrow distribution around $\langle\psi\rangle$ in the film, the formula is given in eq 1 for an unpolarized light geometry.

$$\sin^2\langle\psi\rangle = \frac{2A_{surf}}{3A_{soln}} \quad (1)$$

Because the sulfonate in the zirconium−sulfonate bond can be replaced by a stronger binder—phosphate buffers (HPO_3^{2-}/PO_3^{3-}; pH 11)—we designed the following experiments. Azobenzene chromophores first underwent self-organization from solution onto the surface, and subsequently returned to solution by *quantitative* exchange with a phosphate salt. By examining the starting solution, surface-bound state, and end solution, we obtained the following information: (1) the azobenzene dyes were intact in the process of self-assembling as well as disassembling; (2) surface coverage was determined accurately using the end solution and the Beer−Lambert law $\Gamma_{surf} = A\epsilon^{-1}$; and (3) molecular orientation was experimentally deduced by comparing the absorbance of the surface-bound species to the absorbance of the same amount of that species in the end solution.

Figure 1 shows the molecular orientation deduced from eq 1 versus surface coverage for the chromophoric SAMs. As illustrated in Figure 1, the formation of SAMs can be divided into three categories: partially ordered submonolayers, well-ordered monolayers, and randomized aggregates. When the surface coverage was low, submonolayers were formed with some net alignment. As the surface coverage increased, highly ordered mesoscale structures started to organize and the optimized alignment, $\langle\psi\rangle = 32 \pm 3°$, was achieved while the surface coverage approached a close-packed state of ~2.0−4.0 molecules per nm^2. Aggregation formed on surfaces when the surface coverage was greater than a monolayer and the orientation was random ($\sin^2\langle\psi\rangle = {}^2/_3$). This shows that the average molecular orientation is a complex function of the surface coverage and resulting steric interactions of adjacent rod-like molecules.

Our studies further show that chlorosilane forms better organized thin films than trimethoxysilanes (smaller $\langle\psi\rangle$ at optimum coverage), which agrees with the fact that hydrolysis of chlorosilanes with silanols is more selective than that of methoxysilanes. The optimum surface coverage (minimum points in Figure 1) is governed by the cross-sectional area of the molecule on surfaces. For example, the optimum coverage of AABDS and Sulfarsazene is approximately 1.6 times that of Orange I (3.7 molecules/nm^2 *vs* 2.3 molecules/nm^2), consistent with the molecular cross-section ratio of 1.5, which is due to the bulky naphthanyl group and its steric hindrance effect (Scheme 1).

Second harmonic generation (SHG) was carried out to verify the chromophoric alignment. In the SAM symmetry (C_∞), there are only two independent elements of the second-order nonlinear susceptibility, d_{33} and $d_{31} = d_{32}$. To determine the values of the second-order nonlinear susceptibility, the ratio of d_{33} to d_{31} was first derived by comparison of the angular dependence of the measured p-polarized SHG from p-polarized fundamental *versus* s-polarized fundamental. Molecular orientation $\langle\psi\rangle$ can be deduced by fitting the experimental angular dependence to a theoretical model.[2b] The values obtained for $\langle\psi\rangle$ from these measurements were similar for all of the compounds, within

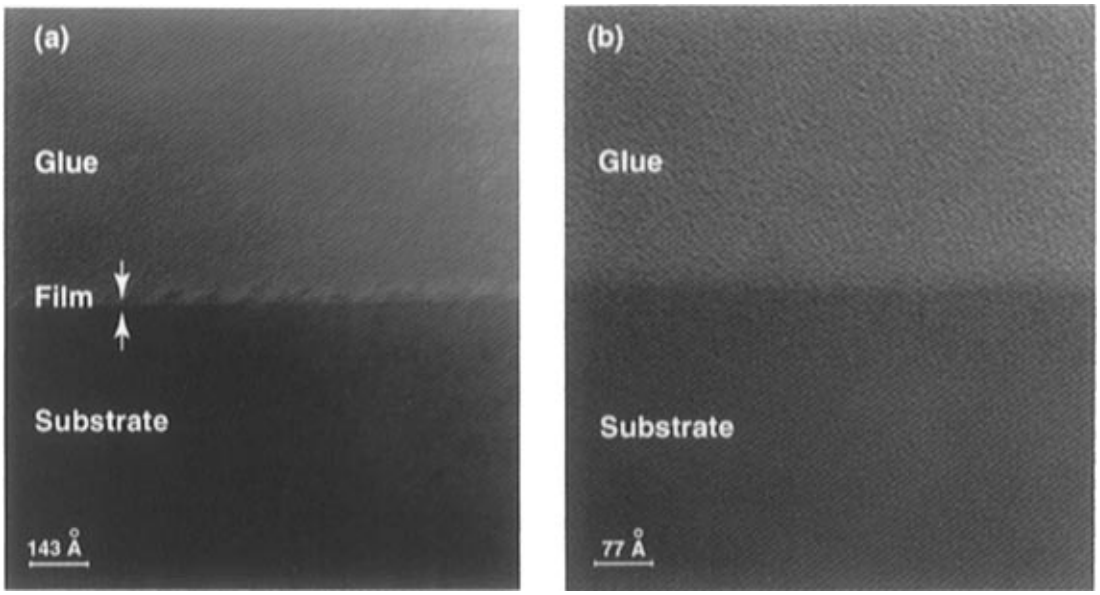

Figure 2. A cross-sectional TEM view of (a) a self-assembled NiPc monolayer on a quartz surface which yields a film thickness of 4.3 ± 0.2 nm; and (b) a quartz and glue interface without film.

the experimental resolution: $\langle\psi\rangle = 35° \pm 5°$. The relatively large uncertainty results from the sensitivity of the deduced molecular orientation angle to the linear optical constants of the thin films, which have not been independently measured; for our fitting we fixed the linear index of refraction at 1064 nm to be 1.5, a typical value for organic molecules at this wavelength.[2b] These results confirm the formation of oriented, polar monolayer films. Values of the second-order nonlinear susceptibility d_{33} relative to crystalline quartz were obtained for SAMs of Orange I, AABDS, Tropaeolin, and Sulfarsazene, respectively; these values were 6.56, 3.88, 6.04, and 1.17 pm/V, respectively.

Cross-sectional TEM imaging was employed to determine the film thickness of NiPc SAMs on quartz. NiPc was chosen because of its robustness and resistance to irradiation of electron beam. Figure 2a shows a cross-sectional TEM image of the as-grown film of a NiPc SAM on quartz with a thickness of 4.3 ± 0.2 nm. This is consistent with the thickness of 3.8 nm calculated from a space-filling model. In contrast, a non-film cross-section TEM image (Figure 2b) exhibits only a flat interface between the substrate and glue. Although the atomic structure cannot be identified, evidence of periodic structure along the film indicates the possibility of crystalline regions; no growth strain can be observed along the interface of the substrate. These data represent the first *direct* observation of a SAM film with 2-Å resolution.[8]

Conclusions

To summarize, we have illustrated the intrinsic relationship between surface coverage and chromophoric orientation in SAMs. The ordering of these SAMs arises from complex intermolecular forces and improves with increasing surface coverage until a monolayer is formed at optimal alignment. Subsequent addition leads to randomly-oriented aggregates. The optimum alignment was found to be $\langle\psi\rangle = 32°$ relative to the surface normal. SHG and TEM studies confirmed the alignment and thickness of the chromophoric SAMs.

Acknowledgment. This work was performed under the auspices of the DOE. We thank Basil I. Swanson for programmatic support. The technical assistance by D. Logsdon and W. Archer is greatly appreciated.

JA9528590

(8) For indirect observation of SAM and the surface native oxide layer on silicon, see the following: (a) Shin, H.; Collins, R. J.; De Guire, M. R.; Heuer, A. H.; Sukenik, C. N. *J. Mater. Res.* **1995**, *10(3)*, 692−8. (b) Shin, H.; Collins, R. J.; De Guire, M. R.; Heuer, A. H.; Sukenik, C. N. *J. Mater. Res.* **1995**, *10(3)*, 699−703.